Transport and diffusion on a body-centered-cubic bcc(110) surface under a constant external force

Katja Lindenberg[a], A. M. Lacasta[b], J. M. Sancho[c] and A. H. Romero[d]

[a] Department of Chemistry and Biochemistry 0340, and Institute for Nonlinear Science, University of California, San Diego, La Jolla, California 92093-0340, USA
[b] Departament de Física Aplicada, Universitat Politècnica de Catalunya, Avinguda Doctor Marañon 44, E-08028 Barcelona, Spain
[c] Departament d'Estructura i Constituents de la Matèria, Facultat de Física, Universitat de Barcelona, Diagonal 647, E-08028 Barcelona, Spain
[d] Cinvestav-Queretaro, Libramiento Norponiente No 2000, Real de Juriquilla, 76230 Queretaro, Qro, Mexico

ABSTRACT

We present a numerical study of classical particles obeying a Langevin equation moving on a solid bcc(110) surface. The particles are subject to a two dimensional periodic and symmetric potential of rectangular symmetry and to an external dc field along one of the diagonals of the structure. One observes a bias current with a component orthogonal to the dc field. The drift velocity (magnitude and direction) and diffusion of the particle depend on the surface potential and external field parameters, the temperature, and the friction coefficient. We numerically explore these dependences. Because the potential perceived by a particle as well as its friction coefficient depend on the nature of the particle, so might the angle between the particle velocity and the dc field. This scenario may thus provide a useful particle sorting technique.

Keywords: Surface, transport, diffusion, external field, sorting

1. INTRODUCTION

The motion of atoms, vacancies, excitations, molecules, clusters of molecules and colloidal particles on surfaces is an active area of research due to its theoretical interest and technological relevance. One area of recent activity (experimental, numerical, and theoretical) concerns the observation that even for large clusters of molecules, long jumps spanning many lattice sites may in some cases be the dominant contributor to the motion.[1–12] In recent work[13,14] we have suggested that these long, even Lévy-like, motions can be described by ordinary Langevin dynamics and do not require the input of any extraordinary assumptions about the driving fluctuations.

A related avenue of extensive investigation has dealt with the transport properties of particles in a symmetric periodic potential subject not only to thermal effects but also to external forces. This interest lies in the extensive range of important physical applications that include Josephson junctions,[15,16] superionic conductors,[17] adsorbates on crystal surfaces,[12,18,19] colloidal spheres,[20–22] and polymers diffusing at interfaces[23] among many others.[24] A constant external force produces a so-called "tilted potential" or "tilted washboard potential," and the further addition of a periodic force gives rise to the "rocked tilted potential".[24–26]

A rather different but theoretically related area of recent activity surrounds a variety of sorting phenomena when mesoscopic particles in a thermal bath and in the presence of an external force or flow field move on a surface modeled as a periodic two dimensional potential. This work is motivated by recent experiments in colloidal transport on a two-dimensional periodic potential landscape generated with an array of optical tweezers,[20–22]

Further author information: Send correspondence to K.L.
K.L. E-mail: klindenberg@ucsd.edu, Telephone: +1 858 534 3285
A.M.L. E-mail:anna@fa.upc.es, Fax: + 34 93 401 77 00
J.M.S.: E-mail: jmsancho@ecm.ub.es, Telephone: +34 93 402 1183
A.H.R. E-mail: aromero@qro.cinvestav.mx, Telephone: + 52 442 441 4909

Noise in Complex Systems and Stochastic Dynamics III, edited by Laszlo B. Kish, Katja Lindenberg, Zoltán Gingl, Proc. of SPIE Vol. 5845 (SPIE, Bellingham, WA, 2005) · 0277-786X/05/$15 · doi: 10.1117/12.610125

and in DNA separation using microfabricated technology.[27,28] Sorting is possible when the direction of motion of the particles deviates from that of the external force or flow field with a deviation angle that depends on particle characteristics, most notably particle size. Sorting of a mixture of particles is then possible through collection at different angles. The efficiency of these sorting devices depends on the particle interactions with the surface, the external forces, and the temperature. We have recently presented a description and analysis of many of the observed phenomena, again on the basis of ordinary Langevin dynamics.[29]

The models mentioned above primarily focus on potential wells arranged in a square lattices. If an external force in such a lattice points along a symmetry axis (e.g. along [1,0] or [0,1]), the particle current will simply follow the direction of the force.[26,29] Note that these symmetry axes are also directions along which potential minima are connected via saddle points. While it is interesting to characterize the velocity and dispersion of the particles in this case,[26] there is no possibility of a component of the particle current in any other direction, and therefore sorting of particles is not possible with this force. A deviation of the direction of motion of the particles from that of the force on a square lattice requires that the force *not* point along a symmetry axis.[29]

In this paper we investigate the direction and dispersion of particle motion when we change the geometry of the lattice. In particular, we choose a bcc geometry described below and again point a dc field along a direction that connects potential minima via saddle points, i.e., a diagonal (which, as we will see, is not a symmetry axis). We show the appearance of a current component perpendicular to the applied force, and study the relative magnitudes of the parallel and perpendicular components and their dispersions as a function of various parameters of the system. Since there is a nonzero angle between the force and the particle current, we note that sorting is in principle possible in this system. This work thus provides some insight into the effects of lattice geometry on these phenomena.

In Sec. 2 we present the model. Our numerical results are presented and explained in Sec. 3. We end with a summary in Sec. 4.

2. THE MODEL

The motion of a collection of non-interacting classical Brownian particles of mass m in this scenario is described by a standard Langevin equation in a two-dimensional periodic potential $V(x,y)$ of characteristic length scales λ_x and λ_y driven by an external force $\boldsymbol{f}(t)$ in the presence of thermal noise and the associated dissipation. The equations of motion for the components (x,y) of the position vector $\boldsymbol{r}$ are

$$\begin{aligned} m\ddot{x} &= -\frac{\partial}{\partial x}V\left(\frac{x}{\lambda_x},\frac{y}{\lambda_y}\right) - \mu\dot{x} + f_x + \xi_x(t) \\ m\ddot{y} &= -\frac{\partial}{\partial y}V\left(\frac{x}{\lambda_x},\frac{y}{\lambda_y}\right) - \mu\dot{y} + f_y + \xi_y(t), \end{aligned} \tag{1}$$

where a dot denotes a derivative with respect to t. The parameter μ is the phenomenological coefficient of friction, and the $\xi_i(t)$ are mutually uncorrelated white (thermal) noises that obey the equilibrium fluctuation-dissipation relation,

$$\langle \xi_i(t)\xi_j(t')\rangle = 2\mu k_B T\delta_{ij}\delta(t-t'). \tag{2}$$

In our previous work we set the length scales equal to one another ($\lambda_x = \lambda_y \equiv \lambda$), which we do in this paper as well) and chose a square lattice with both dc and ac forces along a direction in which the minima of the potentials are connected by saddle points. For a square lattice this is a symmetry axis (e.g., along the [1,0] direction).[26] In the context of sorting phenomena on a square lattice, we considered a dc force along an arbitrary direction explicitly away from this symmetry direction so as to obtain a particle current that deviates from the direction of the force.[29] Here we look at a different lattice geometry. In particular, we choose the periodic potential

$$V(x,y) = V_0\left[1+\sin\left(\frac{2\pi x}{\lambda}\right)\sin\left(\frac{2\pi y}{\sqrt{2}\lambda}\right)\right]. \tag{3}$$

V_0 is the height of the saddle point barriers located at $x = j\lambda/2$ and $y = k\lambda/\sqrt{2}$ for all integer pairs (j,k). This potential can represent a bcc(110) surface,[30] and is shown in Fig. 1. As one can see in the figure, the minima

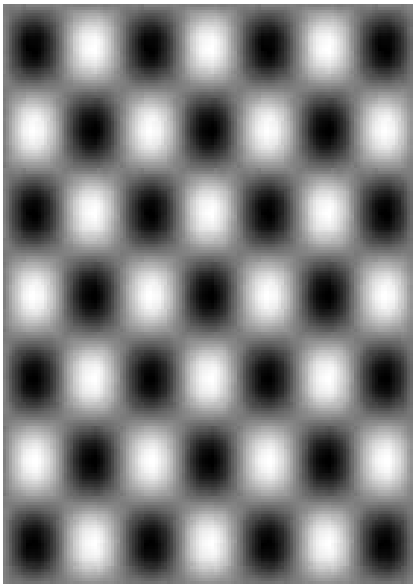

Figure 1. Two dimensional potential Eq. (3) used for our simulations. Black/white areas correspond to maxima/minima.

are connected by saddle points along the diagonals, which in this case are not orthogonal. Thus these diagonals are not symmetry axes of the system (while the x and y directions are). Throughout this work we choose the constant external force $\boldsymbol{f}$ to lie along a diagonal.

The equations of motion for this system can be written in terms of the scaled dimensionless variables

$$r_x = x/\lambda, \qquad r_y = y/\lambda \qquad \tau = \sqrt{V_0}t/\sqrt{m}\lambda \tag{4}$$

as follows:

$$\begin{aligned} \ddot{r}_x &= -\frac{\partial}{\partial r_x}\mathcal{V}(r_x, r_y) - \gamma\dot{r}_x + F_x + \zeta_x(\tau) \\ \ddot{r}_y &= -\frac{\partial}{\partial r_y}\mathcal{V}(r_x, r_y) - \gamma\dot{r}_y + F_y + \zeta_y(\tau). \end{aligned} \tag{5}$$

A dot denotes a derivative with respect to τ, $\mathcal{V}(r_x, r_y)$ is the dimensionless potential, and the scaled noise obeys the fluctuation-dissipation relation

$$\langle \zeta_i(\tau)\zeta_j(\tau')\rangle = 2\gamma\mathcal{T}\delta_{ij}\delta(\tau - \tau'). \tag{6}$$

This scaling serves to stress the fact that for a fixed potential there are only three independent parameters in this model: the scaled temperature $\mathcal{T}$, the scaled dissipation γ, and the scaled magnitude F of the external force, given respectively by

$$\mathcal{T} = \frac{k_B T}{V_0}, \qquad \gamma = \frac{\mu\lambda}{\sqrt{mV_0}}, \qquad F = \frac{f\lambda}{V_0}. \tag{7}$$

Note that since the potential can be generated analytically and the equations of motion are continuous, the system is infinite and it is not necessary to specify any particular boundary conditions.

3. NUMERICAL RESULTS

The observables of interest to us are the mean particle velocity and the diffusion tensor that reflects the spread in the particle trajectories. The averages below indicated by brackets $\langle\cdot\rangle$ are over thermal fluctuations and over

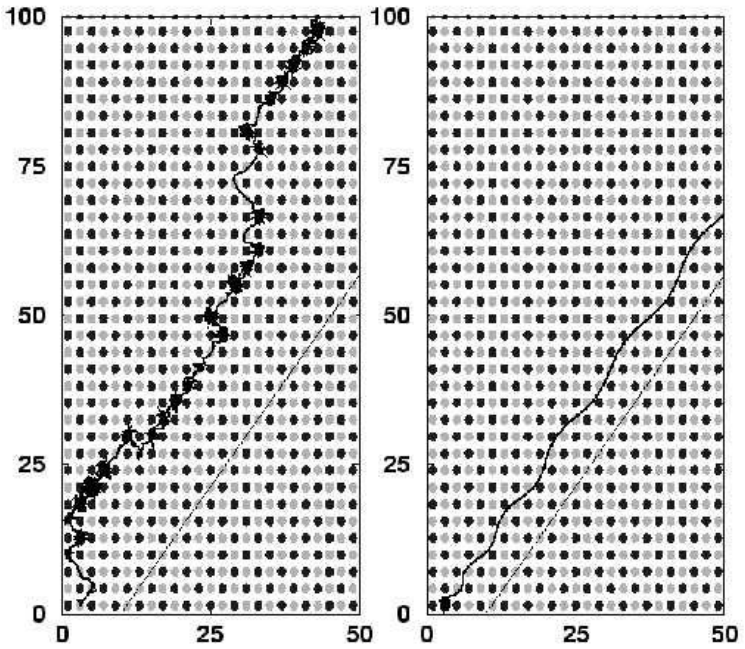

Figure 2. Typical realizations of trajectories in the presence of a constant force along a system diagonal. Parameter values: $\lambda = 4$, $\mathcal{T} = 0.2$ and $F = 0.8$. Left panel: $\gamma = 2$. The angle between the force and the average velocity is approximately 10°. Right panel: $\gamma = 0.2$. The average velocity and force are essentially parallel.

an ensemble of particles. We define the mean velocity component along direction u as

$$v_u = \lim_{\tau\to\infty} \frac{\langle r_u \rangle}{\tau}, \qquad r_u = \boldsymbol{r}(t).\boldsymbol{u}, \tag{8}$$

where $\boldsymbol{r}(t)$ is the particle displacement and $\boldsymbol{u}$ is a unit vector that we choose to lie either parallel or perpendicular to $\boldsymbol{F}$. The diffusion coefficients of interest are

$$D_u = \lim_{\tau\to\infty} \frac{\langle [r_u(\tau) - \langle r_u(\tau)\rangle]^2]\rangle}{2\tau}. \tag{9}$$

In particular, when u is parallel (perpendicular) to the external dc force we call the associated quantities $v_\parallel$ ($v_\perp$), and $D_\parallel$ ($D_\perp$).

We study these observables as a function of the strength of the force for different friction coefficients and for different temperatures. As noted earlier, one of the most interesting features of this problem is that the particle trajectory deviates from the direction of the force when the latter lies along a system diagonal. We highlight this deviation in our discussion.

Underlying the appearance of a component of the velocity perpendicular to the applied force along a lattice diagonal is the following physical picture, clearly illustrated by the typical trajectories shown in Fig 2. The straight solid line is the force along a diagonal. A particle is pulled by the force, and along the way it falls into subsequent wells from which it emerges as a result of thermal fluctuations which allow it to move over saddle points connecting the wells. While the particle preferentially moves forward following the force, it is nevertheless also attracted to wells in the direction of the other diagonal. On occasion the thermal fluctuations allow it to overcome the preferential direction imposed by the force. Since the diagonals are not orthogonal, this off-line motion preferentially occurs to one side of the force direction. After such a detour the motion along the force resumes, until an off-line step occurs once again. In the figure the force points along the left-to-right diagonal and as a result the off-line motions occur preferentially toward the left. Clearly, in the higher friction realization in

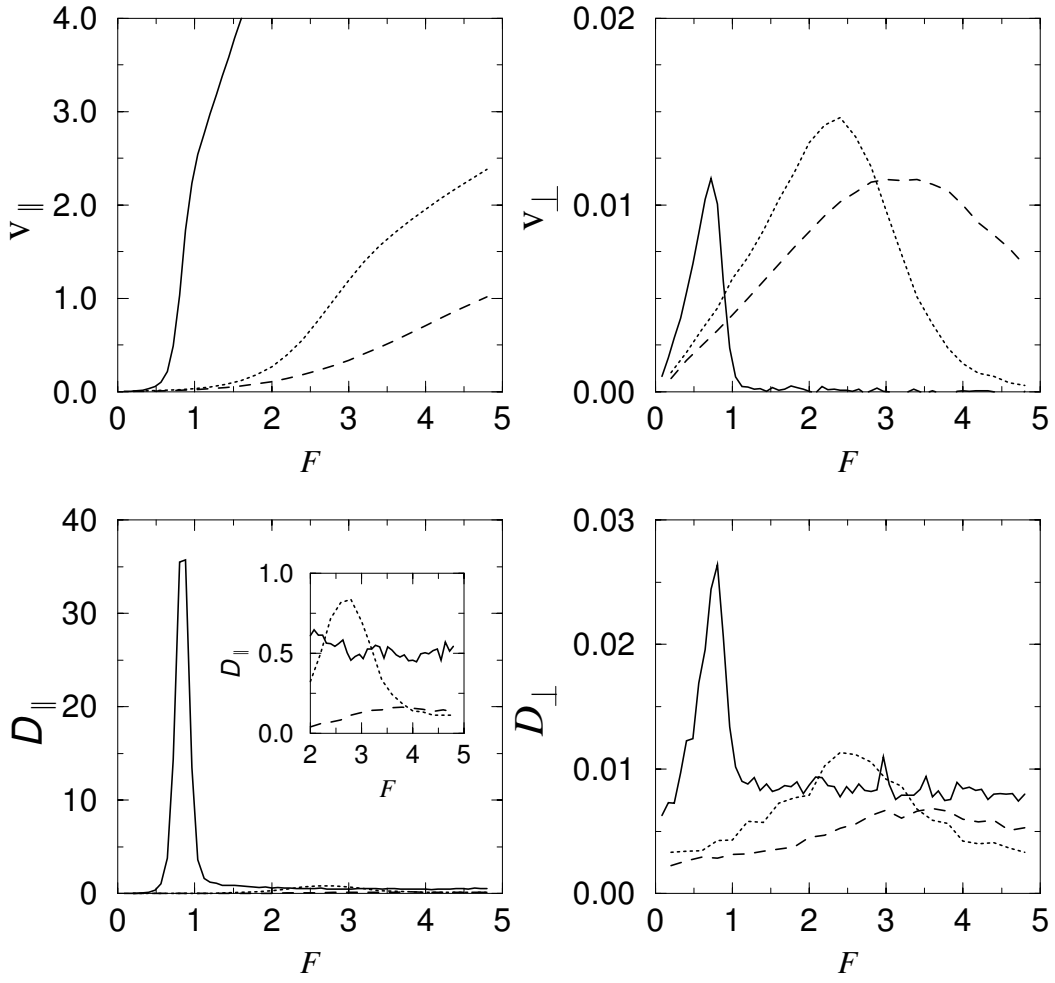

Figure 3. $v_\parallel$, $v_\perp$, $D_\parallel$, and $D_\perp$ vs F. Results shown are for different friction coefficients: $\gamma = 0.4$ (solid), $\gamma = 2$ (dotted), and $\gamma = 4$ (dashed). The temperature is $\mathcal{T} = 0.2$. The inset in the third panel expands the scale so that the variations of $D_\parallel$ can be seen for all three cases.

addition to the velocity component along the force, the particle also acquires a velocity component perpendicular to the force. Also clearly, the velocity deviation is strongly dependent on friction, a dependence we return to later. While we expect the parallel components of the velocity and diffusion tensor not to be too strongly affected by geometry, that is, to be similar to those observed in a square lattice with a force along a symmetry axis,[26] the components perpendicular to the direction of the force should be sensitive to this geometry (and are in fact nonzero only because of the geometry).

Next, in Fig. 3, we present results for the velocity and diffusion tensor components as a function of F for various friction coefficients. The first panel shows the dependence of $v_\parallel$ on F for different values of the friction coefficient. The dependences here are quite similar to those encountered in a system of ordinary square geometry and a force along a symmetry axis, and can be understood as follows.[24, 26] At very low forces the particle does not move, i.e., it is locked in place. At very high forces, the particle is simply pulled along by the force. The interesting nonlinear regimes occur at intermediate forces, determined by the friction coefficient. In the high friction case the unlocking occurs when the tilt of the surface potential produced by the external force is sufficiently large for the minima of the potential to disappear; the transition thus occurs when the minima become marginally stable states (or, for large but finite friction, near this point), and is insensitive to the value

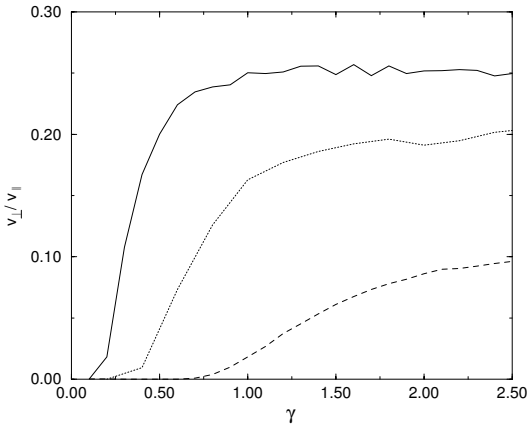

Figure 4. $v_\parallel/v_\perp$ as a function of friction for different values of the force: $F = 0.4$ (solid), $F = 0.8$ (dotted), and $F = 1.6$ (dashed). The temperature is $\mathcal{T} = 0.2$.

of the friction. The particle thus acquires net motion when there are no potential barriers. In the low friction case the particles have inertia and can therefore escape the potential wells into a running state even while there are still potential minima. However, the depth of the well where this becomes possible is sensitively dependent on the friction, since it involves a balance between the loss of energy due to friction and the gain in kinetic energy due to the external force. This leads to a transition that sets in at lower forces and leads to higher velocities in the low friction case than in the high friction case. The third panel in Fig. 3 shows the parallel component of the diffusion tensor, whose behavior is again similar to that found in a system of square geometry, and the peak and width can be understood as follows.[24,26] A typical particle trajectory moves randomly from locked to running back to locked, and so on. During a locked interval the velocity is zero, and diffusion around zero velocity is typically small. During a running interval the velocity is not zero, and again the diffusion around the nonzero velocity is typically small. As a result the apparent diffusion about the *average* velocity $v_\parallel$ may be large, somewhat artifically, because this average velocity is not the most probable velocity of a particle. In other words, in this regime the velocity distribution is *bimodal* rather than unimodal about the average velocity,[24,26,31] and the calculated $D_\parallel$ is the full width of this bimodal distribution and not reflective of the width of each of the two modes. Note that the increased diffusion is consistent with the linear response theory result for a free particle that associates D with v through the derivative relation $D = k_B\mathcal{T}dv/dF$. Our particle is neither free, nor is the force in the transition region particularly small, but nevertheless large diffusion is associated with a steep slope of velocity vs F that here comes about because of switching between different velocities. With increasing friction the transition region moves to higher forces and becomes less abrupt. The associated maximum of the diffusion coefficient then also moves to higher forces and becomes less pronounced.

The new features are the perpendicular components of the velocity and diffusion tensor. The second panel in Fig. 3 shows the perpendicular mean velocity component for various values of the friction. A number of features are noteworthy. First, this velocity component vanishes at zero force (when the particle does not move) and at large force (when the particle simply gets dragged along in the direction of the force), and peaks between these two extremes. The position of the optimal force for perpendicular motion essentially coincides with the force at which the variation of the parallel component of the force is greatest, and therefore also with the force where $D_\parallel$ also peaks. The fourth panel shows the corresponding perpendicular diffusion coefficient $D_\perp$. The peak here is again associated with the regime of greatest variation in both velocity components as well as in the parallel diffusion tensor component. Again, these peaks reflect the parameter regime where there are frequent transitions between the locked and running regimes of particle motion.

For particle sorting purposes one is interested in the ratio $v_\perp/v_\parallel$, which here is different for different friction coefficients (hence providing, in principle, a tool to separate particles with different friction coefficients). As a function of F for a fixed γ this ratio is essentially monotonically decreasing, which is consistent with the results

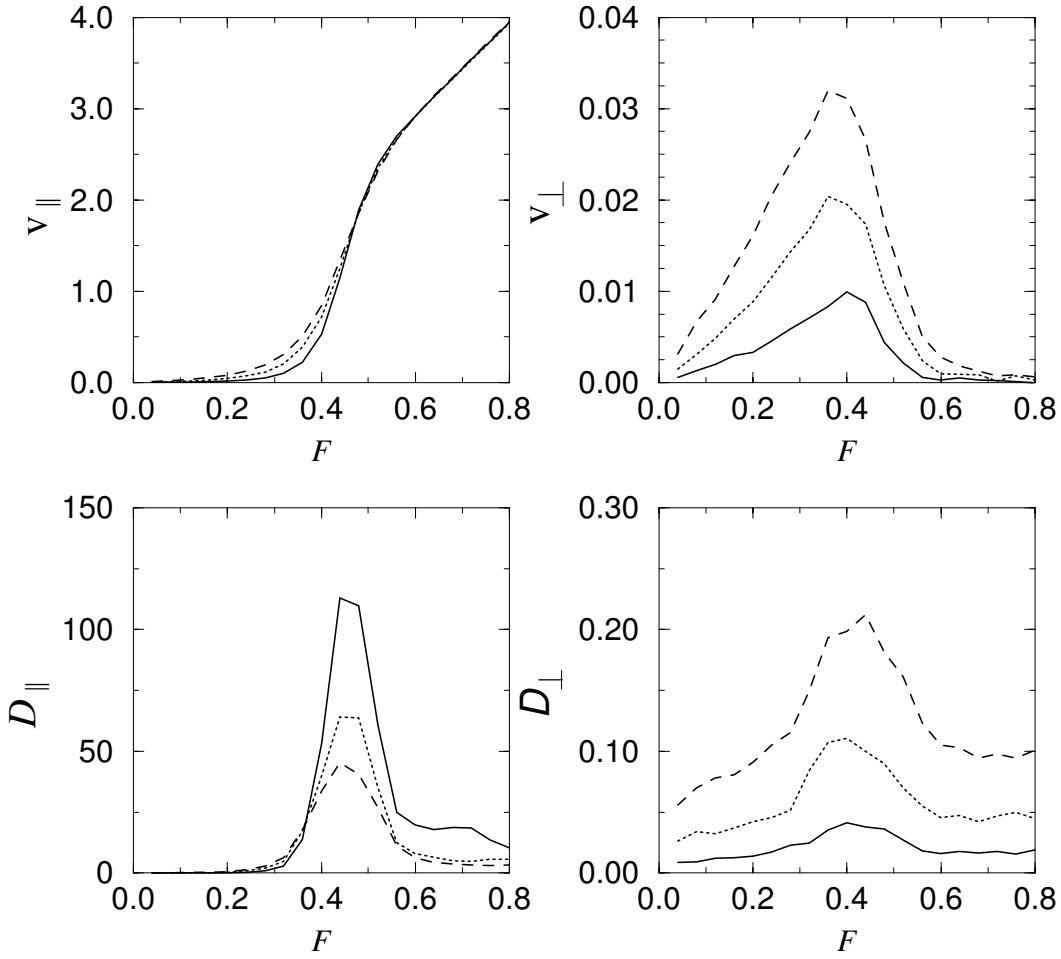

Figure 5. $v_\parallel$, $v_\perp$, $D_\parallel$, and $D_\perp$ vs F for different temperatures: $\mathcal{T} = 0.2$ (solid), $\mathcal{T} = 0.25$ (dotted), and $\mathcal{T} = 0.3$ (dashed). The friction coefficient is $\gamma = 0.2$.

in Fig. 3. As a function of γ for different values of the force, the ratio is shown in Fig. 4 (compare with the trajectories in Fig. 2. It increases from zero and asymptotes at a value that depends on the force. Note that for the parameters used to generate the trajectories in Fig. 2 the ratio $v_\perp/v_\parallel$ is vanishingly small for the lower friction, where inertia plays an important role leading to long particle jumps between trapping events, and where the fluctuations are weak. The ratio is nearly 0.2 for the higher friction, which corresponds to the angle of approximately 10° quoted in the trajectory figure.

Interesting behavior is evident when we examine the velocity and diffusion tensor as a function of temperature for low friction, as shown in Fig. 5. The first and third panels showing the parallel components again behave in a way similar to the velocity and diffusion coefficient in a square lattice when the force is applied along the [1,0] direction. The principal effect on $v_\parallel$ of lowering the temperature is to sharpen the transition region, essentially without moving its location. The center of the transition region, regardless of temperature, is located near the value of F that defines the abrupt transition as temperature goes to zero. However, the effect on the diffusion coefficient is far more pronounced. While the location of the peak is essentially temperature independent, as we would expect from the fact that the velocity transition remains localized around the same value of the force, the peak *grows* with *decreasing* temperature, that is, diffusion is *stronger* as temperature decreases, again consistent with the sharpening of the velocity transition. This behavior is consistent with our earlier description of the

diffusion in the switching region between locked and running states.

We have already noted why the perpendicular velocity component vanishes at low and high forces and therefore (given that it can be nonzero) peaks in between. The position of the peak is fairly insensitive to temperature changes, consistent with the reasoning for the parallel component. The height of the peak, on the other hand, here depends strongly on and decreases with increasing temperature, i.e., increasing temperature tends to counteract the effect of geometry. This is reasonable, since increasing thermal fluctuations would tend to diminish the difference in the "up" and "down" motions illustrated in the trajectory of Fig. 2. The perpendicular component of the diffusion tensor again peaks at a location that is insensitive to temperature changes, as with all the other quantities discussed above, but again the height of the peak now increases with increasing temperature.

4. SUMMARY

We have presented a numerical study of the motion of Brownian particles on a bcc(110) surface with a dc force along a diagonal defined by potential wells connected by saddle points. Because this is not a symmetry axis of the lattice, the resulting current of particles develops a component perpendicular to this direction, $v_\perp$, in addition to the parallel component $v_\parallel$, so that the net average motion of the particles is not parallel to the applied force. The deviation angle between the force and the particle current depends on the parameters of the model, notably the friction coefficient, thus pointing to a procedure to separate particles with different friction coefficients. We studied the behavior of the mean velocity components $v_\parallel$ and $v_\perp$ as a function of the applied force, the temperature, and the friction coefficient. There is dispersion about each of these components due to thermal fluctuations, and we also studied the associated diffusion tensor components $D_\parallel$ and $D_\perp$ as a function of applied force, temperature, and friction coefficient. While our analysis is so far only numerical, we are able to provide qualitative explanations for the observed behaviors.

ACKNOWLEDGMENTS

This work was supported by the Engineering Research Program of the Office of Basic Energy Sciences at the U. S. Department of Energy under Grant No. DE-FG02-04ER46179, by the MCyT (Spain) under project BFM2003-07850, by CONACyT–México through grant J-42647-F, and by a grant from the University of California Institute for México and the United States (UC MEXUS) and the Consejo Nacional de Ciencia y Tecnología de México (CONACyT).

REFERENCES

1. D. C. Senft and G. Ehrlich, "Long jumps in surface diffusion: One-dimensional migration of isolated adatoms," *Phys. Rev. Lett.* **74**, p. 294, 1995.
2. T. R. Linderoth, S. Horch, E. Laegsgaard, I. Stensgaard, and F. Besenbacher, "Surface diffusion of Pt on Pt(110): Arrhenius behavior of long jumps," *Phys. Rev. Lett.* **78**, p. 4978, 1997.
3. A. P. Graham, F. Hofmann, J. P. Toennies, L. Y. Chen, and S. C. Ying, "Experimental and theoretical investigation of the microscopic vibrational and diffusional dynamics of sodium atoms on a Cu(001) surface," *Phys. Rev. B* **56**, p. 10567, 1997.
4. S.-M. Oh, , S. J. Koh, K. Kyuno, and G. Ehrlich, "Non-nearest-neighbor jumps in 2d diffusion: Pd on W(110)," *Phys. Rev. Lett.* **88**, p. 236102, 2002.
5. W. D. Luedtke and U. Landman, "Slip diffusion and Lévy flights of an adsorbed gold nanocluster," *Phys. Rev. Lett.* **82**, p. 3835, 1999.
6. J. Wecksesser, J. V. Barth, C. Cai, B. Mueller, and K. Kern, "Binding and ordering of large organic molecules on an anisotropic metal surface: PVBA on Pd(110)," *Surf. Sci.* **431**, p. 168, 1999.
7. M. Schunack, T. R. Linderoth, F. Rosei, E. Laengsgaard, I. Stendgaard, and F. Besenbacher, "Long jumps in the surface diffusion of large molecules," *Phys. Rev. Lett.* **88**, p. 156102, 2002.
8. G. Ertl and H.-J. Freund, "Catalysis and surface science," *Phys. Today* **52**, p. 32, 1999.
9. G. Antczak and G. Ehrlich, "Long jump rates in surface diffusion: W on W(110)," *Phys. Rev. Lett.* **92**, p. 166105, 2004.
10. Y. Goergievskii and E. Pollak, "Semiclassical theory of activated diffusion," *Phys. Rev. E* **49**, p. 5098, 1994.

11. Y. Goergievskii and E. Pollak, "Long hops of an adatom on a surface," *Surf. Sci.* **355**, p. L366, 1996.
12. E. H. E, P. Talkner, E. Pollak, and Y. Goergievskii, "Multiple hops in multidimensional activated surface diffusion," *Surf. Sci.* **421**, p. 73, 1999.
13. J. M. Sancho, A. M. Lacasta, K. Lindenberg, I. M. Sokolov, and A. H. Romero, "Diffusion on a solid surface: Anomalous is normal," *Phys. Rev. Lett.* **92**, p. 250601, 2004.
14. A. M. Lacasta, J. M. Sancho, A. H. Romero, I. M. Sokolov, and K. Lindenberg, "From subdiffusion to superdiffusion of particles on solid surfaces," *Phys. Rev. E* **70**, p. 051104, 2004.
15. G. Barone and A. Paterno, *Physics and Applications of the Josephson Effect*, John Wiley and Sons, New York, 1982.
16. R. L. Kautz, "Noise, chaos, and the josephson voltage standard," *Rep. Prog. Phys.* **59**, p. 935, 1996.
17. W. Dieterich, P. Fule, and I. Peschel, "Theoretical models for superionic conductors.," *Adv. Phys.* **29**, p. 527, 1980.
18. J. W. M. Frenken and J. F. V. der Veen, "Observation of surface melting," *Phys. Rev. Lett.* **54**, p. 134, 1985.
19. B. Pluis, A. W. D. van der Gon, J. W. M. Frenken, and J. F. van der Veen, "Crystal-face dependence of surface melting," *Phys. Rev. Lett.* **59**, p. 2678, 1987.
20. P. Korda, M. B. Taylor, and D. G. Grier, "Kinetically locked-in colloidal transport in an array of optical tweezers," *Phys. Rev. Lett.* **89**, p. 128301, 2002.
21. A. Gopinathan and D. G. Grier, "Statistically locked-in transport through periodic potential landscapes," *Phys. Rev. Lett.* **92**, p. 130602, 2004.
22. M. P. MacDonald, G. C. Spalding, and K. Dholakia, "Microfluidic sorting in an optical lattice," *Nature* **426**, p. 421, 2003.
23. G. I. Nixon and G. W. Slater, "Entropic trapping and electrophoretic drift of a polyelectrolyte down a channel with a periodically oscillating width," *Phys. Rev. E* **53**, p. 4969, 1996.
24. H. Risken, *The Fokker-Planck Equation, Chapter 11*, Springer Verlag, New York, 1989.
25. M. Borromeo and F. Marchesoni, "A.c.-driven jump distributions on a periodic substrate," *Surf. Sci.* **465**, p. L771, 2000.
26. K. Lindenberg, A. M. Lacasta, J. M. Sancho, and A. H. Romero, "Transport and diffusion on crystalline surfaces under external forces," *New. J. of Phys.* **7**, p. 29, 2005.
27. L. R. Huang, E. C. Cox, R. H. Austin, and J. C. Sturm, "Tilted Brownian ratchet for DNA analysis," *Anal. Chem.* **75**, p. 6963, 2003.
28. L. R. Huang, E. C. Cox, R. H. Austin, and J. C. Sturm, "Continuous particle separation through deterministic lateral displacement," *Science* **304**, p. 987, 2004.
29. A. M. Lacasta, J. M. Sancho, A. H. Romero, and K. Lindenberg, "Sorting on periodic surfaces," *sumbitted for publication* , 2005.
30. L. Y. Chen, M. R. Baldan, and S. C. Ying, "Surface diffusion in the low-friction limit: Occurrence of long jumps," *Phys. Rev. B* **54**, p. 8856, 1996.
31. G. Costantini and F. Marchesoni, "Threshold diffusion in a tilted washboard potential," *Europhys. Lett.* **48**, p. 491, 1999.